

# Cramér-Rao Bound for Intravoxel Incoherent Motion Diffusion Weighted Imaging Fitting \*

Qinwei Zhang, *Student Member, IEEE*, Yi-Xiang Wang, Heather Ting Ma, *Member, IEEE*, Jing Yuan\*, *Senior Member, IEEE*

**Abstract**—The precision of parameter estimation for Intravoxel Incoherent Motion Diffusion Weighted Imaging (IVIM-DWI) was investigated by examining their Cramér-Rao bounds (CRBs) under the presence of Rician noise. Monte Carlo (MC) simulation was also conducted to validate the CRB results. The estimation uncertainties of true diffusion coefficient ( $D$ ) and perfusion fraction ( $f_0$ ) could reach 3.89% and 11.65% respectively with typical parameter values at a moderate signal-to-noise ratio (SNR) of 40. However, to estimate pseudo diffusion coefficient ( $D^*$ ) within 10% uncertainty requires  $\text{SNR} > 122$ . The results also showed that the estimation precision of each parameter is not only dependent on SNR but also their true values, while this mutual dependency is complicated. Under some particular cases, estimation uncertainty for certain parameters might be smaller than 5% at a moderate SNR of 40. However, the simultaneous precise estimation for all three parameters is theoretically difficult and highly SNR demanding.

## I. INTRODUCTION

Diffusion Weighted Imaging (DWI) that reflects the random microscopic motion of water protons has been widely applied in clinics. Image intensity ( $S$ ) of DWI is traditionally described by a mono-exponential decay model,

$$S = S_0 \cdot e^{-b \cdot ADC} \quad (1)$$

where  $b$  is the so-called b-factor that is determined by diffusion-weighted gradient strength and duration;  $ADC$  is the apparent diffusion coefficient;  $S_0$  is the image intensity with  $b=0$  s/mm<sup>2</sup>;

During recent years, numerous studies have found that under some circumstances the measured DWI intensity  $S$  against  $b$  deviated from the mono-exponential decay. Instead, DWI signal attenuation can often be described by a bi-exponential model, which is written as [1-3],

$$S_{biexp} = S_0 [f_0 \exp(-bD^*) + (1 - f_0) \exp(-bD)], \quad (2)$$

where  $D^*$  and  $D$  are two distinct diffusion coefficients and  $f_0$  and  $(1 - f_0)$  are their corresponding fractions.

Two biophysical models have been proposed to explain the bi-exponential DWI signal. The first model attributes the two diffusion coefficients to the intra-cellular (slow diffusion)

and extra-cellular free water (fast diffusion) components. The bi-exponential decay becomes detectable at very high  $b$  factor, typically  $b > 2500$  s/mm<sup>2</sup> [4]. The second model is termed as Intravoxel Incoherent Motion (IVIM), proposed by Le Bihan [5]. In IVIM, the microcirculation within the randomly oriented capillary network is considered as pseudo-diffusion with a much larger diffusion coefficient ( $D^*$ ) than the normal true diffusion coefficient ( $D$ ). IVIM effect has been found in many well-perfused tissues at low  $b$  values ( $< 200$  s/mm<sup>2</sup>). IVIM offers a novel method for simultaneous and non-invasive perfusion and diffusion imaging and has arisen increasing research interest in the recently years.

Accurate and precise quantification of bi-exponential parameters is important but still challenging for the characterization of tissue properties, particularly at low signal-to-noise ratio (SNR). The Cramér-Rao Bound (CRB) sets the theoretical lowest limit on the variance of the estimated parameters for any un-biased estimators [6, 7]. In this study, we examine the CRB of bi-exponential parameters for the IVIM model under the presence of Rician distributed noise, and compare the CRB to the uncertainty of the estimated parameters by using non-negative least-square (NNLS) method though Monte Carlo simulation. This study is helpful to predict the theoretically achievable precision for bi-exponential parameter quantification and the optimization of acquisition protocol for IVIM imaging.

## II. THEORY AND METHOD

### A. Cramér-Rao Bound

Suppose the parameters to be estimated are  $\vec{\beta}$ , and the likelihood function is  $L$ , which represents the probability of the occurrence of a certain observation. Thus, the Fisher information matrix  $\vec{F}$  can be written as

$$\vec{F} = E \left[ \left( \frac{\partial \ln(L)}{\partial \beta} \right)^T \left( \frac{\partial \ln(L)}{\partial \beta} \right) \right]. \quad (3)$$

Here  $E[\cdot]$  stands for the expectation operator. If  $\vec{\xi}$  is an unbiased estimator of  $\vec{\beta}$ , then the covariance of  $\vec{\xi}$  has the property as

$$\text{Cov}(\vec{\xi}, \vec{\xi}) \geq \vec{F}^{-1}. \quad (4)$$

The right hand of the inequality is the CRB. Eq. (4) shows that the variance of the elements in  $\vec{\xi}$  is always not smaller than the corresponding diagonal elements of the CRB [8]. CRB serves as a useful tool to quantify the theoretical highest precision achievable by an unbiased estimator.

\*Research supported by Hong Kong GRC grant CUHK418811, CUHK475911 and SEG\_CUHK02.

Q. Zhang, Y-X Wang and J. Yuan\* (corresponding author) are with the Department of Imaging and Interventional Radiology, The Chinese University of Hong Kong, Shatin, NT, Hong Kong, China (phone: 852-2632-1036; fax: 852-2636-0012; e-mail: jyuan@cuhk.edu.hk). J. Yuan is also with the CUHK Shenzhen Research Institute. H. T. Ma is with Harbin Institute of Technology Shenzhen Graduate School.

### B. Cramér-Rao Bounds expression of IVIM-DWI

It is known that the noise in MR magnitude images is governed by Rician distribution [9] under single-coil acquisition, whose probability density function (PDF) is given by

$$P_{\text{Rician}}(M, \mathbf{S}_{\text{biexp}}, \sigma) = \frac{M}{\sigma^2} e^{-\left[\frac{M^2 + \mathbf{S}_{\text{biexp}}^2}{2\sigma^2}\right]} I_0\left(\frac{M \mathbf{S}_{\text{biexp}}}{\sigma^2}\right), \quad (5)$$

where  $\sigma^2$  is the noise variance and  $\mathbf{S}_{\text{biexp}}$  is the true signal intensity without noise as given by Eq. (2).  $M$  is the measured signal intensity, i.e. the observation.  $I_0$  is the 0<sup>th</sup> order modified Bessel function. Every single observation  $M_n$  corresponding to a  $b$ -value can be written as,

$$M_n = \mathbf{S}_{\text{biexp}}(b_n, \vec{\beta}) + r_n. \quad (6)$$

Here  $\vec{\beta} = (f_0, D^*, D)$ .

Estimation of  $\vec{\beta}$  is conducted by finding the maximum value of  $L$ :

$$\frac{\partial \ln(L)}{\partial \vec{\beta}} = \vec{0}. \quad (7)$$

Combined with Eq. (5),  $\vec{F}$  of the parameters  $\vec{\beta}$  can be obtained by [8].

$$\vec{F} = \left(\frac{\partial \mathbf{S}_{\text{biexp}}(\vec{\beta})}{\partial \vec{\beta}}\right)^T \tilde{V}^{-1} E[\tilde{R}] \left(\frac{\partial \mathbf{S}_{\text{biexp}}(\vec{\beta})}{\partial \vec{\beta}}\right). \quad (8)$$

$\tilde{V}^{-1}$  is a diagonal matrix with elements  $\frac{1}{\sigma_n^2}, \dots, \frac{1}{\sigma_n^2}$ .  $E[\tilde{R}]$  is also a diagonal matrix with element given by

$$E[\tilde{R}]_{n,n} = -\frac{\mathbf{S}_{\text{biexp}}^2}{\sigma_n^2} + E\left[\frac{M_n^2 I_1(M_n \mathbf{S}_{\text{biexp}} / \sigma_n^2)}{\sigma_n^2 I_0(M_n \mathbf{S}_{\text{biexp}} / \sigma_n^2)}\right]. \quad (9)$$

Then the first, second and third diagonal element of  $\vec{F}^{-1}$  are the CRB of  $f_0$ ,  $D^*$  and  $D$  respectively. Numerical integration is used to compute  $E[\tilde{R}]$ . At high SNR, where Rician distribution approaches Gaussian distribution,  $E[\tilde{R}]$  turns into a unit matrix.

### C. Cramér-Rao Bounds Computation

A set of typical IVIM parameter values were investigated at first,  $f_0 = 0.1$ ,  $D^* = 0.02$  mm<sup>2</sup>/s and  $D = 0.001$  mm<sup>2</sup>/s.

Without losing generality,  $S_0$  was set as 1. CRBs were computed on different SNRs, from 5 to 200. SNR was defined as the ratio of the  $S_0$  and the noise standard deviation, i.e.,  $1/\sigma$ . A  $b$ -factor combination that was frequently used in practice was adopted as [0, 20, 40, 50, 60, 80, 100, 150, 200, 400, 600, 800, 1000] s/mm<sup>2</sup>. The estimation uncertainty of CRB was evaluated by the ratio of the square root of CRB, i.e. SD, and the corresponding true value.

We further computed the CRBs for SNRs (from 5 to 100) over a much wider range of these three parameters (one parameter varied, and the other two fixed),  $f_0$  from 0.05 to 0.65;  $D^*$  from 0.015 to 0.075 mm<sup>2</sup>/s;  $D$  from 0.0005 to 0.006 mm<sup>2</sup>/s. Finally, the dependence of CRB uncertainty on each varying parameter was also investigated for a fixed SNR of 40, a clinically achievable typical value.

### D. Monte Carlo simulation.

Monte Carlo (MC) simulation was conducted and the results were compared with the CRB. Rician noise was generated according to the pre-assigned SNRs and imposed on the noiseless data determined by Eq. (4) with the true parameter values to produce the noisy data. The noisy data was then fitted by using the non-negative least-squares (NNLS) algorithm to obtain the estimated bi-exponential parameters. This procedure repeated 10,000 times for each bi-exponential parameter set. The standard deviation of all estimated parameters ( $n=10,000$ ) divided by the corresponding true parameter value, named the uncertainty of MC, was compared to the uncertainty of CRB obtained with the parameter sets for different SNRs. All computations involved in CRB and MC simulation were conducted in Matlab (The MathWorks, Natick, MA) with homemade scripts.

## III. RESULTS AND DISCUSSION

The CRB uncertainty of  $f_0$ ,  $D^*$  and  $D$  were all found decay with the increase of SNR in the uncertainty order of  $D < f_0 < D^*$ , as shown by red dash lines in Fig. 1. The estimated  $D$  was the most precise, with the uncertainty of CRB equaled 33.32% at SNR=5, and 0.78% at SNR=200, while the estimation of  $D^*$  was highly uncertain, with the uncertainty from 247.23% to 6.10%. The precision of  $f_0$  was in-between, with the corresponding uncertainty varied from 95.51% to 2.33%. The SNR were 15.5 and 46.5 for  $D$  and  $f_0$  at which

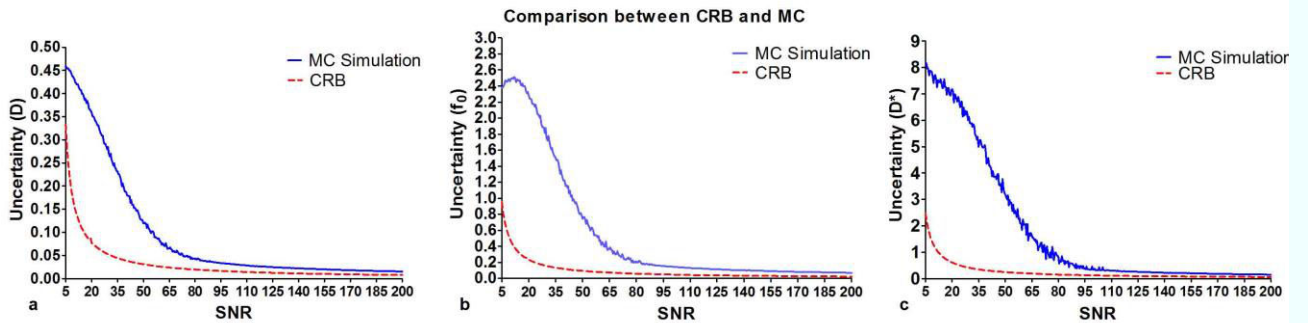


Fig. 1. Uncertainties of CRB and MC (give values) for  $D$  (a),  $f_0$  (b) and  $D^*$  (c) at different SNRs from 5 to 200. Results illustrate the uncertainty order:  $D < f_0 < D^*$ . The values in MC results were much higher than CRB at SNR < 80, and then approached to CRB.

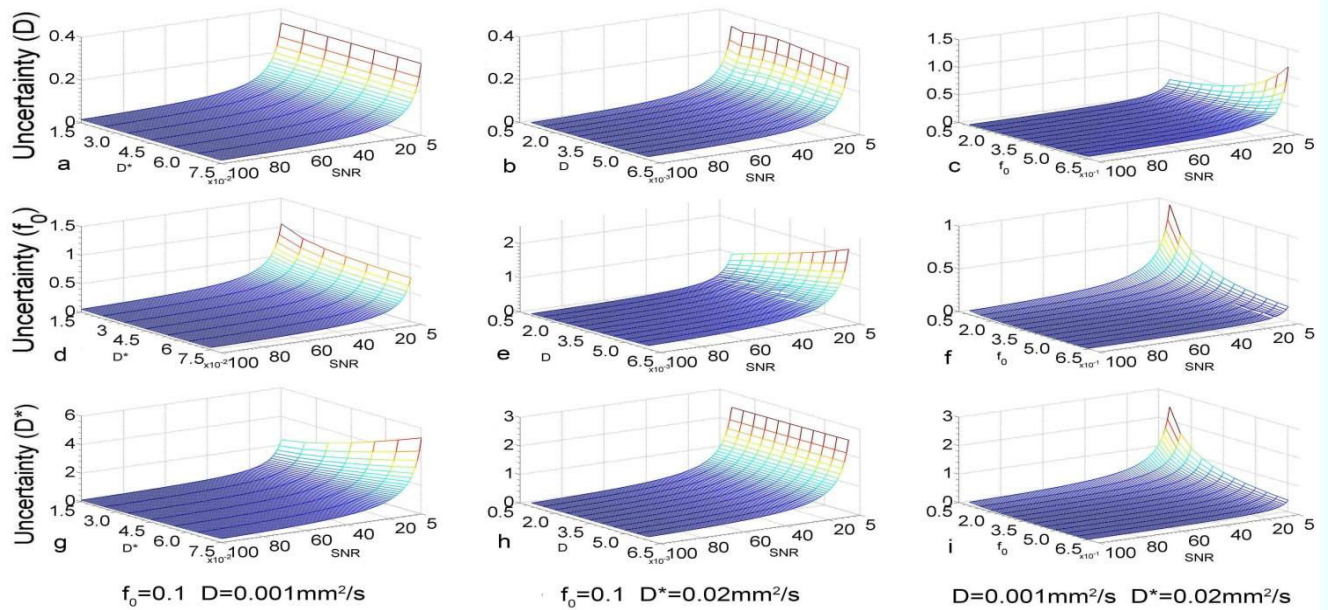


Fig. 2. CRB results of estimation uncertainty with different parameter values and SNRs. All parameter uncertainties decreased with the increase of SNR.

their uncertainty reached 10%, which were usually achievable for clinical examination. However, to obtain the same precision for  $D^*$ , the SNR should be above 122, usually unachievable in practice within reasonable scan time. For SNR=40, the uncertainties were 3.89%, 11.65% and 30.49% for  $D$ ,  $f_0$  and  $D^*$  respectively. Furthermore, the CRB results indicated the estimation uncertainty reduced rapidly at SNR<20, and then decreased slowly. These results were consistent with previous study[10].

The blue lines in Fig. 1 depict the uncertainty of MC simulation. The uncertainties were much higher than CRB results when the SNR was below 80. With even higher SNRs, the MC results approached CRB results, which validated the CRB results very well.

Fig. 2 illustrates the CRB of each parameter varied with SNR. As comparison, Fig. 3 illustrates the uncertainty of MC simulation correspondingly. The variation trends of uncertainty were generally consistent with CRB results in Fig. 2. The MC uncertainty was higher than that for CRB except for a few data points at low SNRs (Fig. 3 e, h). These data points with unexpected low uncertainty in Fig. 3 may be caused by the initial value and fitting bound setting in NNLS estimation, which would lead to significantly biased underestimation or overestimation at low SNR. The CRB results at SNR=40 were depicted in Fig.4, showing the dependence of estimation uncertainty on the variation of true parameter values. The uncertainty of  $D$  was insensitive to  $D^*$  (a, c), while it dropped with the decrease of  $f_0$  and the increase of  $D$  when  $D$  was small (b). The uncertainty was

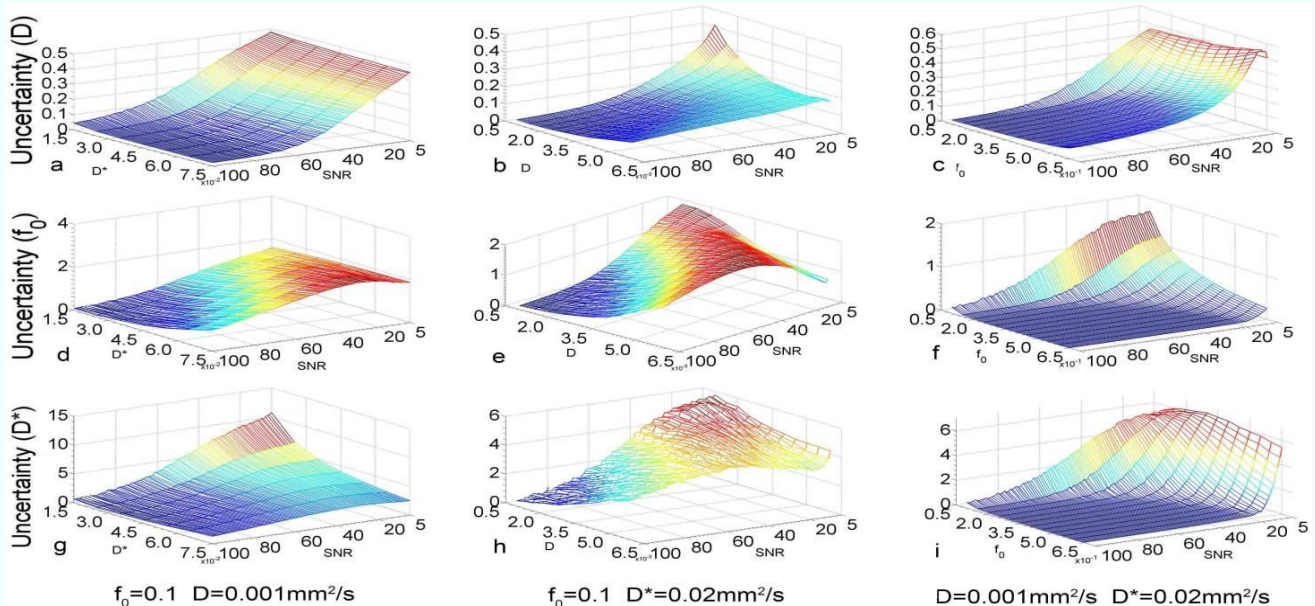


Fig. 3. MC simulation results of estimation uncertainty with different parameter values and SNRs. The variation trends of uncertainty were consistent with CRB results in Fig. 2.

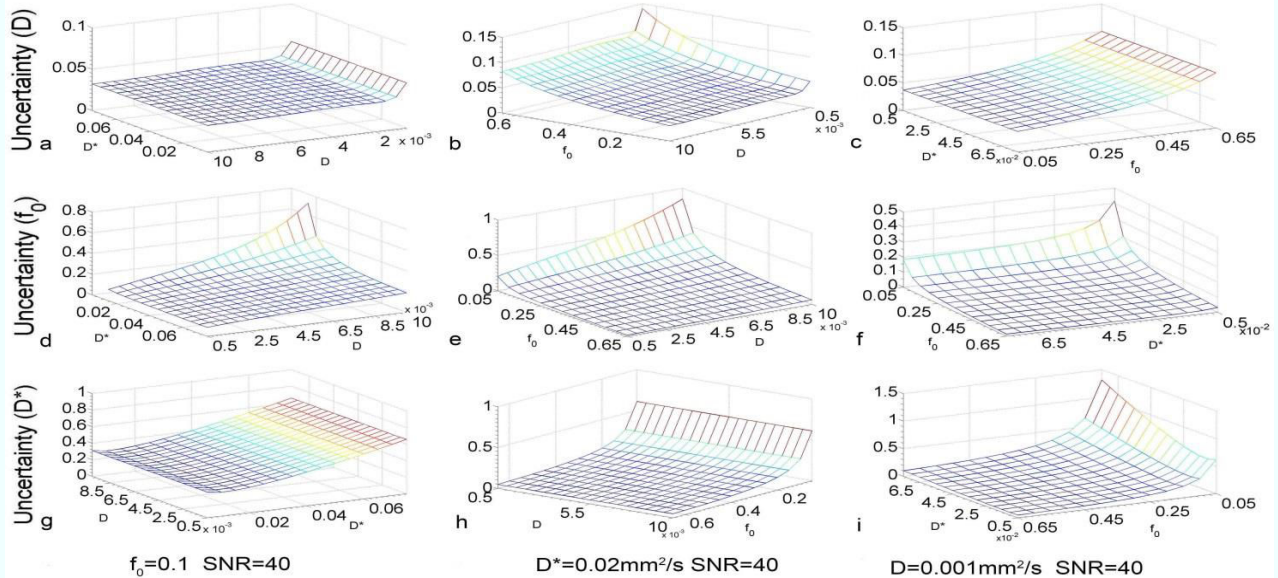


Fig. 4. CRB results of different parameter values and fixed SNR. Estimation uncertainties have difference dependencies on parameters. Certain parameter may be precisely estimated (uncertainty<5%) under particular situations.

only 3.2% at  $f_0=0.05$ ,  $D=0.006\text{mm}^2/\text{s}$  (b). The uncertainty of  $f_0$  (d, e, f) was dependent on every parameter. It increased rapidly with the increasing  $D$  for small  $D^*$  (d) and  $f_0$  (e). As seen from (f), the precise estimation of  $f_0$  was more difficult when its true value was very small, e.g.  $f_0<0.1$ , particularly for  $D^*<1.5\times 10^{-2}\text{mm}^2/\text{s}$ . The uncertainty of  $D^*$  dropped with the increase of  $f_0$  (h, i) and the decrease of  $D^*$  (g), while relatively independent of  $D$  (g, h). It had the lowest value of 4.7% at  $f_0=0.65$ ,  $D^*=0.005\text{mm}^2/\text{s}$  (i). According to Fig. 4, certain parameter may be precisely estimated (uncertainty<5%) at clinical achievable SNR under particular situations, e.g., the estimated  $D^*$  should be quite precise if  $f_0$  is large ( $f_0>0.6$ ). However, the simultaneous precise estimation of all three parameters could be still challenging at the moderate SNR=40.

This study has some limitations. This study only studied the IVIM-DWI parameter estimation contaminated by Rician noise. However, the noise profiles may deviate from Rician distribution under multi-coil acquisition and parallel imaging. The CRBs under these conditions should be further investigated. Furthermore, only one b-value set was investigated in this study, which may not be the best acquisition scheme. Nevertheless, the investigation of CRBs for different b-value sets is helpful for the acquisition optimization to pursuit lower uncertainties. Experiments are warranted in the future to validate the theoretical results derived from this study.

#### IV. CONCLUSION

The precision of IVIM estimation was analyzed quantitatively by examining the theoretical CRBs. Several conclusions could be drawn: for some particular parameter values, precise estimation of  $D$  and  $f_0$  could be achieved at moderate SNRs, while estimation of  $D^*$  was much more SNR demanding. Second, the precision of parameter estimation is strongly dependent on SNR and their true values, while this dependency can be complicated. As a thumb of rule, precise

estimation of  $D$  requires high  $D$  and low  $f_0$  values; precise  $f_0$  estimation requires high  $D^*$ ,  $f_0$  and low  $D$  values; precise  $D^*$  estimation requires high  $f_0$  and low  $D^*$  values. It is always worth noting that the true values of IVIM parameters are primarily determined by the intrinsic properties of tissues. Therefore, the difficulties of precise estimation of IVIM parameters vary with different tissues in practice. Further studies are warranted for the improvement of IVIM parameter quantification.

#### REFERENCES

- [1] T. Niendorf, R. M. Dijkhuizen, D. G. Norris, M. V. Campagne, and K. Nicolay, "Biexponential diffusion attenuation in various states of brain tissue: Implications for diffusion-weighted imaging," *Magnetic Resonance in Medicine*, vol. 36, pp. 847-857, Dec 1996.
- [2] R. V. Mulkern, H. Gudbjartsson, C.-F. Westin, H. P. Zengingonul, W. Gartner, C. R. G. Guttman, et al., "Multi-component apparent diffusion coefficients in human brain†," *NMR in Biomedicine*, vol. 12, pp. 51-62, 1999.
- [3] C. A. Clark and D. Le Bihan, "Water diffusion compartmentation and anisotropy at high b values in the human brain," *Magnetic Resonance in Medicine*, vol. 44, pp. 852-859, Dec 2000.
- [4] R. V. Mulkern, S. J. Haker, and S. E. Maier, "On high b diffusion imaging in the human brain: ruminations and experimental insights," *Magn Reson Imaging*, vol. 27, pp. 1151-62, Oct 2009.
- [5] D. M. Koh, D. J. Collins, and M. R. Orton, "Intravoxel incoherent motion in body diffusion-weighted MRI: reality and challenges," *AJR Am J Roentgenol*, vol. 196, pp. 1351-61, Jun 2011.
- [6] C. R. Rao, "Minimum variance and the estimation of several parameters," in *Mathematical Proceedings of the Cambridge Philosophical Society*, 1947, pp. 280-283.
- [7] H. Cramer, *Mathematical Methods of Statistics (PMS-9)* vol. 9: Princeton university press, 1999.
- [8] O. T. Karlsen, R. Verhagen, and W. M. Bovee, "Parameter estimation from Rician-distributed data sets using a maximum likelihood estimator: application to T1 and perfusion measurements," *Magn Reson Med*, vol. 41, pp. 614-23, Mar 1999.
- [9] H. Gudbjartsson and S. Patz, "The Rician Distribution of Noisy Mri Data," *Magnetic Resonance in Medicine*, vol. 34, pp. 910-914, Dec 1995.
- [10] J. Pekar, C. T. W. Moonen, and P. C. M. Vanzijl, "On the Precision of Diffusion Perfusion Imaging by Gradient Sensitization," *Magnetic Resonance in Medicine*, vol. 23, pp. 122-129, Jan 1992.